Dissipative and hysteresis loops as images of irreversible processes in nonlinear acoustic fields

C. M. Hedberg[1] and O. V. Rudenko[1,2,3,4,a)]
[1]*School of Engineering, Blekinge Institute of Technology, Karlskrona 371 79, Sweden*
[2]*Department of Physics, Moscow State University, Moscow 119991, Russia*
[3]*Prokhorov General Physics Institute of the Russian Academy of Sciences, Moscow 119991, Russia*
[4]*Shmidt Institute of Earth Physics of the Russian Academy of Sciences, Moscow 123995, Russia*

(Received 13 March 2011; accepted 1 August 2011; published online 6 September 2011)

Irreversible processes taking place during nonlinear acoustic wave propagation are considered using a representation by loops in a thermodynamic parameter space. For viscous and heat conducting media, the loops are constructed for quasi-harmonic and sawtooth waves and the descriptive equations are formulated. The linear and nonlinear absorptions are compared. For relaxing media, the processes are frequency-dependent. The loops broadens, narrows, and bends. The linear and nonlinear relaxation losses of wave energy are shown. Residual stresses and irreversible strains appear for hysteretic media, and here, a generalization of Rayleigh loops is pictured which takes into account the nonlinearly frequency-dependent hereditary properties. These describe the dynamic behavior, for which new equations are derived. © *2011 American Institute of Physics*. [doi:10.1063/1.3631800]

I. INTRODUCTION

Irreversibility in acoustics is created by a variety of processes. Even a weak linear wave loses energy through viscosity and heat conductivity, due to molecular absorption and relaxation processes, scattering, emission, and many of the other mechanisms.[1,2] For nonlinear waves, additional mechanisms of energy loss appear, becoming stronger with increase in the intensity.[3–7] The nonlinear losses depend not only on the wave amplitude, but on the gradients of acoustic field, i.e., on its spatiotemporal structure. The description of losses by thermodynamic cycles (loops) in a stress-strain or a pressure-volume diagram is well-known. Commonly, loops exist for dissipative and hysteresis processes. The structural features of loops for nonlinear waves have, as far as we know, not been treated earlier. The loops form a pictorial rendition of the irreversible processes. In this paper, it will be demonstrated that this method gives a deeper understanding of the physical distinctions between the different irreversible processes accompanying the nonlinear propagation of high-intensity acoustic waves.

II. A VISCOUS AND HEAT CONDUCTING MEDIUM

Consider a certain unit mass in a fluid, in other words a "liquid particle." The change of internal energy of this particle is given by the thermodynamic identity[2]

$$dU = \theta\, ds + p\frac{d\rho}{\rho^2}. \tag{1}$$

For high frequency (fast) acoustic oscillations, the variation of entropy can be neglected: $ds = 0$. Now, let the acoustic field be periodic. Then, the increase in energy (1) during a cycle of vibration is equal to

$$U = \oint p\frac{d\rho}{\rho^2} = \oint \frac{dp}{\rho}. \tag{2}$$

Suppose now that $p = p_0 + p',\ \rho = \rho_0 + \rho'$, where subscript "zero" means the thermodynamic equilibrium parameters. The primed variables are the weak disturbances caused by the acoustic field. For weak and periodic disturbances, the expression (2) takes a form

$$U = -\frac{1}{\rho_0^2}\oint \rho'\, dp' = \frac{1}{\rho_0^2}\oint p'\, d\rho'\,. \tag{3}$$

It is shown below by examples how to derive physically evident results from Eq. (3), in parallel with results for nonlinear waves. It is convenient to use an equation connecting the variations caused by a nonlinear wave in a viscous and heat conducting medium (see Ref. 3, formula (2.1.12))

$$\frac{p'}{c_0^2\rho_0} = \frac{\rho'}{\rho_0} + (\varepsilon - 1)\left(\frac{\rho'}{\rho_0}\right)^2 + \frac{b}{2c_0^2\rho_0^2}\frac{\partial \rho'}{\partial t}. \tag{4}$$

Formula (4) generalizes the algebraic equation of state $p(\rho)$ known for Riemann waves. It was suggested for nonlinear acoustic problems by Khokhlov in 1961 (Ref. 8) (see also Refs. 3 and 9). Some time earlier Khokhlov used a similar equation for nonlinear electromagnetic waves.[10] The formal reason for this generalization was to simplify the derivation of nonlinear evolution equations of Burgers type. However, the physical merits of this "formal substitution" have not been utilized until now. As distinct from the algebraic equation of state $p(\rho)$, formula (4) contains a first time derivative, which leads to the appearance of a time delay. To illustrate this, Eq. (4) can, at weak nonlinearity and weak dissipation, be rewritten in another form

[a)]Author to whom correspondence should be addressed. Electronic mail: rudenko@acs366.phys.msu.ru.

$$\frac{\rho'(t)}{\rho_0} = -(\varepsilon-1)\left(\frac{p'}{c_0^2\rho_0}\right)^2 + \frac{1}{\tau_T}\int_{-\infty}^{t}\frac{p'(t')}{c_0^2\rho_0}\exp\left(-\frac{t-t'}{\tau_T}\right)dt',$$

here, $\tau_T = b/(c_0^2\rho_0)$ is the "transport time" which for weakly decaying adiabatic sound waves of the frequency ω satisfies the inequality $\omega\tau_T \ll 1$. One can see that the appearance of the exponential kernel is caused by the time derivative in formula (4). Consequently, formula (4) can be referred to as a "constitutive equation" rather than an "equation of state" implying an instantaneous relation of variables. However, at $\omega\tau_T \ll 1$, the finite time delay described by the integral term cannot be realized. This term transforms at $\omega\tau_T \ll 1$ to a $(\omega\tau_T)^n$ power series (n = 1, 2, 3…), whose two first terms

$$\frac{1}{\tau_T}\int_{-\infty}^{t}\frac{p'(t')}{c_0^2\rho_0}\exp\left(-\frac{t-t'}{\tau_T}\right)dt' \approx \frac{p'}{c_0^2\rho_0} - \frac{\tau_T}{c_0^2\rho_0}\frac{\partial p'}{\partial t},$$

form a constitutive equation like (4). It means that the finite delay can be described by an infinite power series containing derivatives of arbitrarily large order. Restricting ourselves to the first derivative, we take into account only a small time delay. Effects of large delays are discussed in the subsequent sections.

In formula (4), the following notations are used: ε is the nonlinear coefficient and b is the effective dissipative coefficient expressed in terms of shear and bulk viscosities and thermal conductivity. All notations here are standard for nonlinear acoustics and are the same as the ones used, for example, in the books.[3,4,6,11] By substituting Eq. (4) into Eq. (3), one can derive, after simple transformations, the equation for the increase of internal energy during a period $T = 2\pi/\omega$

$$U = \frac{b}{2\rho_0^3}\int_{t_0}^{t_0+T}\left(\frac{\partial\rho'}{\partial t}\right)^2 dt = \frac{bT}{2\rho_0^3}\overline{\left(\frac{\partial\rho'}{\partial t}\right)^2}, \tag{5}$$

where an overline denotes the average over one period.

An increase in the energy (5) corresponds to increase of the thermal (chaotic) motion. It happens due to a decrease in the energy of the ordered particle motion and is caused by the absorption of the wave. The entropy grows, of course, but this growth is not significant and the isentropic approximation is rather accurate.[2]

It will be shown now that the increment of internal energy (5) is exactly equal to the energy loss of the wave. The propagation along the x-axis is described by Burgers equation[3–7]

$$\frac{\partial u}{\partial x} = \frac{\varepsilon}{c_0^2}u\frac{\partial u}{\partial t} + \frac{b}{2c_0^3\rho_0}\frac{\partial^2 u}{\partial t^2}, \tag{6}$$

here, u is the vibration velocity. Multiplying both sides of Eq. (6) by u and averaging over one period, one can derive the following equation describing the energy loss for a unit mass during a period of oscillation

$$\frac{\overline{u^2}}{2} = -\frac{b}{2c_0^3\rho_0}\int_{x_0}^{x_0+c_0T}\overline{\left(\frac{\partial u}{\partial t}\right)^2}dx. \tag{7}$$

Replace the vibration velocity in the right hand side of Eq. (7) by the density variation using the relation $u = c_0\rho'/\rho_0$ for a plane wave and replace the integration over dx in Eq. (7) by multiplication of the integrand by c_0T. The last action is correct because the shape of wave varies slowly during its propagation over distances on the order of a wavelength. The resulting formula

$$\frac{\overline{u^2}}{2} = -\frac{bT}{2\rho_0^3}\overline{\left(\frac{\partial\rho'}{\partial t}\right)^2}, \tag{8}$$

differs from Eq. (5) only in sign, i.e., $U = -\overline{u^2}/2$. Consequently, the energy loss leads to an equal increment of the internal energy, which was to be proven.

The two most important examples are considered here. When the wave is harmonic in time,

$$\rho' = A(x)\,\sin(\omega t), \tag{9}$$

formula (5) results in

$$U = \frac{\pi}{2}\frac{b}{\rho_0^3}\omega A^2(x). \tag{10}$$

The increase in energy (10) is proportional to the effective viscosity coefficient b of a viscous and heat conducting medium.

In the other limiting case, when the wave is strongly distorted by nonlinearity, it has a sawtooth shape. One period of it is described by Khokhlov's solution[3]

$$\rho' = A(x)\left[-\frac{\omega t}{\pi} + \tanh\left(\frac{\varepsilon c_0^2}{b}A(x)\,t\right)\right], \quad -\pi < \omega t < \pi. \tag{11}$$

Substitute the solution (11) into Eq. (5) for the increase of internal energy over one period. Let the medium have low viscosity and a high acoustic Reynolds number.[3] For this case, the duration of shock front is small in comparison with the period, and energy absorption is localized to the vicinity of the shock front. A calculation with a high Reynolds number approximation results in

$$U = \frac{2}{3}\frac{\varepsilon c_0^2}{\rho_0^3}A^3(x). \tag{12}$$

Let us compare Eqs. (10) and (12). If nonlinear absorption predominates (Eq. (12)), the increase of energy U depends neither on the duration of the period T (or on the frequency ω), nor on the effective viscosity b and U is proportional to the cube of the amplitude $A^3(x)$. At the same time, for a linear absorption $U \sim A^2(x)$ (10). Note, that Eqs. (10) and (12) are applicable not only to plane waves, but for any one-dimensional wave. They are valid for spherical and cylindrical waves, waves in horns and concentrators, as well as inside ray tubes when geometrical acoustic is used to describe high-frequency waves. For each particular case the expression for $A(x)$ has to be stated.[12]

Let us pass now to the construction of $p' \Leftrightarrow \rho'$ diagram for a viscous heat conducting medium by means of Eq. (4). For a linear or weakly nonlinear wave having a near harmonic profile (9), one can exclude time and derive an analytical equation

$$\left[Y - X - (\varepsilon - 1)\frac{A}{\rho_0}X^2\right]^2 + \beta^2 X^2 = \beta^2. \qquad (13)$$

For simplicity, the following notations are used

$$Y = \frac{p'}{c_0^2 A}, \quad X = \frac{\rho'}{A}, \quad \beta = \frac{b\omega}{2c_0^2\rho_0}. \qquad (14)$$

The loops described by Eq. (13) are shown in Fig. 1(a): without account for the nonlinear term (dashed curve); and with account for nonlinearity (solid curve). One can see that the linear loop has an elliptic form, but nonlinearity deforms this loop to a crescent. The area of this loop is completely determined by the number β which is proportional to dissipation b.

At strongly expressed nonlinearity, the wave profile contains shock fronts and the shape of the wave is far from harmonic. In this case, an exact explicit expression for the loop $p'(\rho')$ cannot be derived. However, the loop can be constructed if Eqs. (4) and (11) are considered as a parametric representation of the curve. Different sections on the loop can be considered separately. For a smooth slope of the wave, where the acoustic density decreases in time according to a linear law (see the first term inside brackets (11)), the lower section of the loop is described by the formula

$$Y_1 = X + (\varepsilon - 1)\frac{A}{\rho_0}X^2 - \frac{\beta}{\pi}. \qquad (15)$$

The upper section corresponding to a time-increasing acoustic density is given by another formula

$$Y_2 = X + (\varepsilon - 1)\frac{A}{\rho_0}X^2 + \frac{\varepsilon}{2}\frac{A}{\rho_0}\left(1 - X^2\right). \qquad (16)$$

This arc is a consequence of Eq. (4) and the second term inside the brackets (11). The loop given by Eqs. (15) and (16) is shown in Fig. 2.

The area inside the curve corresponds to the sum of usual linear absorption and the additional absorption at the shock front. While the pressure and density are decreasing,

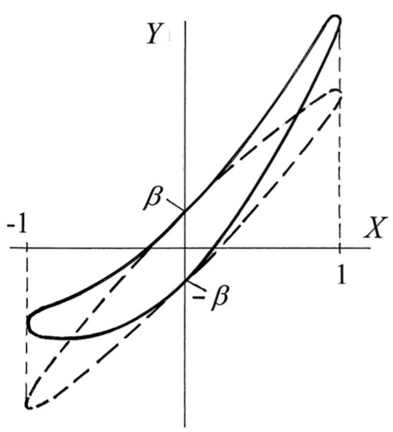

FIG. 1. Dissipative loops at $p' \Leftrightarrow \rho'$ diagram. For a linear wave, the loop has an elliptic form, shown by the dashed line. Quadratic nonlinearity deforms the loop to a crescent, as shown by the solid line.

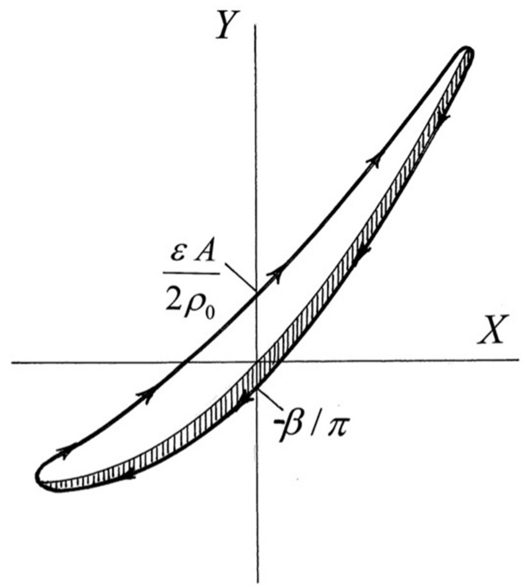

FIG. 2. The loop in a $p' \Leftrightarrow \rho'$ diagram for a sawtooth wave. The smaller shaded area corresponds to the viscous (linear) absorption at smooth sections of the wave profile. The high nonlinear absorption at the shock front corresponds to the (larger) unshaded area.

no additional absorption appears, because in a quadratic nonlinear media a stable rarefaction shock cannot exist.

The result of calculation of internal energy (3) based on Eqs. (15) and (16) reads

$$U = \frac{c_0^2}{\rho_0^2}A^2\int_{-1}^{1}(Y_2 - Y_1)\,dX = \frac{2}{3}\frac{\varepsilon c_0^2}{\rho_0^3}A^3(x) + \frac{b\omega}{\pi\rho_0^3}A^2(x). \qquad (17)$$

The first term in Eq. (17) is equivalent to formula (12) describing a purely nonlinear absorption. The second term in Eq. (17) differs from Eq. (10) only in the coefficient because the smooth section of sawtooth-shaped profile differs from the harmonic profile of linear wave.

III. A RELAXING MEDIUM

The connection between the acoustic equilibrium deviations in pressure and density p', ρ' when internal processes takes place at different time scales, differs from the Eq. (4) and has an integral form[13]

$$\frac{p'}{c_0^2\rho_0} = \frac{\rho'}{\rho_0} + (\varepsilon - 1)\left(\frac{\rho'}{\rho_0}\right)^2 + \int_{-\infty}^{t} K(t - t')\frac{\partial}{\partial t'}\left(\frac{\rho'}{\rho_0}\right)dt'. \qquad (18)$$

The kernel $K(t)$ in the integrand describes the internal dynamics having its own typical times independent from the frequency of the wave. Molecular relaxations, chemical reactions, and energy exchanges between translational degree of freedom and internal degrees of molecules serve as examples of processes which determine the form of $K(t)$. This kernel is responsible for the appearance of dispersion and of frequency dependent absorption. To connect the concrete form of the kernel with the measured characteristics of a medium, the simplest model of a linear plane wave is considered. The corresponding evolution equation[3] is

$$\frac{\partial p}{\partial x} = \frac{1}{2c_0}\frac{\partial^2}{\partial t^2}\int_0^\infty K\left(\frac{\xi}{\tau}\right)p(x,\ t-\xi)\,d\xi.$$

To derive the dispersion law, it is necessary to seek for the solution in the form

$$p = p_0\exp(-i\omega t + ikx), \quad k = k' + ik''.$$

Here k is the wave number and k', k'' are its real and imaginary parts. Substituting the solution into the evolution equation, we find

$$k' = -\frac{\omega^2\tau}{2c}\int_0^\infty K(s)\sin(\omega\tau s)\,ds,$$
$$k'' = \frac{\omega^2\tau}{2c}\int_0^\infty K(s)\cos(\omega\tau s)\,ds.$$

The formula for k' gives a frequency-dependent addition to the velocity of wave propagation: $c(\omega) = c_0(1 - ck'(\omega)/\omega)$. The formula for k'' defines the absorption coefficient of the amplitude $p_0\exp(-k''x)$.

Performing inverse transformations of the formulas for k', k'', one can reconstruct the kernel $K(s)$ for a given medium. The concrete form of a kernel can be calculated on the basis of experimental measurements of frequency-dependent absorption k'' or dispersion k' or on the basis of a corresponding physical model. The standard method[14] of reconstruction exploits the causality principle according to which the two functions k' and k'' cannot be arbitrary but are connected by relations of Kramers-Kronig type.

The method of kernel reconstruction was used, for example, at the derivation of nonlinear models describing medical ultrasound in soft tissues.[15] It is known that the absorption of ultrasound in tissues inside the most interesting frequency range obeys a power law $k'' \sim \omega^{2-\nu}$, $0 < \nu < 1$. It is easy to reconstruct the kernel $K(s) = s^{\nu-1}$ and verify that the corresponding absorption coefficient

$$k'' = \frac{m}{2ct_0}\Gamma(\nu)\cos\left(\frac{\pi}{2}\nu\right)(\omega t_0)^{2-\nu},$$

has the correct frequency dependence. Note that this power kernel has a singularity at $s = 0$ and is not integrable in semi-infinite limits. However, the convolution of this kernel with the oscillating function describing the wave provides for the convergence of the integral for k''. This example demonstrates that a wide variety of applications can be described. Another power kernel $K(s) = 1/\sqrt{s}$ corresponds to friction of a viscous fluid in an acoustic boundary layer. The corresponding integro-differential equation was used to describe energy loss in the neck of Helmholtz resonator,[16] in muscle fibers[17] and for colloidal solutions of nano-particles.[18]

Often the hereditary properties are assumed to be exponential, which means that the memory decays according to an exponential law[3,13]

$$K(t) = m\exp(-t/\tau). \tag{19}$$

Here τ, m are the characteristic time of the memory and the "force" of a relaxation process.

Substitution of Eqs. (18) and (19) into formula (3), it is reduced to the form

$$U = -\frac{m}{c_0^2\rho_0^2\tau}\oint dp'\int_0^\infty p'(t-\xi)\exp\left(-\frac{\xi}{\tau}\right)d\xi. \tag{20}$$

For periodic oscillation another representation can be more convenient

$$U = \frac{mT}{c_0^2\rho_0^2\tau}\sum_{n=1}^\infty(-1)^{n+1}\overline{\left(\tau^n\frac{\partial^n p'}{\partial t^n}\right)^2}. \tag{21}$$

In particular, for a harmonic signal $p' = c_0^2 A\cdot\sin(\omega t)$ in the low-frequency limit ($\omega\tau \ll 1$, when the series (21) is convergent), it follows from Eq. (21) that

$$U = \pi m\frac{c_0^2}{\rho_0^2}\frac{\omega\tau}{1+\omega^2\tau^2}A^2. \tag{22}$$

This result, as is seen from Eq. (20), is valid for arbitrary frequencies in the linear approximation. A comparison of Eqs. (22) and (10) shows that in the low frequency limit, the combination $2mc_0^2\rho_0\tau$ plays the role of an effective dissipation coefficient b.

After passing some distance through the relaxing medium, the wave becomes strongly distorted. Its shock front may then be described by the stationary solution[3]

$$\frac{dX}{dt} = \frac{1-X^2}{2\tau(D+X)}, \quad D = \frac{m}{2\varepsilon}\frac{\rho_0}{A}. \tag{23}$$

The solution (23) is correct for $D > 1$ (Refs. 3 and 11). At $D < 1$, the absorption caused by the relaxation processes cannot prevent the formation of a shock and one has to take both relaxation and viscosity into consideration. Substituting (23) into the first term of Eq. (18) results in the expression

$$U = m\frac{c_0^2}{\rho_0^2}A^2\left[D + \frac{D^2+1}{2}\ln\frac{D+1}{D-1}\right]. \tag{24}$$

At $D = 1$ in the point $X = -1$, the derivative (23) tends to infinity, the shock front has maximum steepness, and the absorption (24) has the maximum strength. The increase in absorption at large values of D is described by Eq. (24). But, it is correct only when the duration of shock front is small in comparison with the period of acoustic oscillation.

We will now construct the thermodynamic loops for relaxing media by analogy with the approaches resulting in Figs. 1 and 2. With the integral connection between acoustic density and pressure (18), the exponential kernel (19) and the Eq. (9), one can derive

$$\left[Y - (1+\varphi_1)X - (\varepsilon-1)\frac{A}{\rho_0}X^2\right]^2 + \phi_2^2X^2 = \phi_2^2. \tag{25}$$

The notations (14) are used here, and

$$\phi_1 = m\frac{\omega^2\tau^2}{1+\omega^2\tau^2}\ , \quad \phi_2 = m\frac{\omega\,\tau}{1+\omega^2\tau^2}\ . \qquad (26)$$

The function φ_1 is responsible for the dispersion of the sound velocity and φ_2 for the frequency-dependent absorption.

Loops (25) are shown in Fig. 3 for three different values of $\omega\tau$: 0.2 (dotted line), 1 (solid line), and 3 (dashed line). The maximum area under the solid curve corresponds to the maximum absorption over one cycle which is found at $\omega\tau = 1$. In both the limiting cases, of $\omega\tau = 0$ and $\omega\tau \to \infty$, the area and, therefore, the absorption tend to zero. With increase in $\omega\tau$, the loop turns counter-clockwise. This turning is due to the growth of sound velocity with increase in $\omega\tau$.

IV. A HYSTERESIS CYCLE

The internal dynamics in a relaxing medium considered in Sec. III is connected with a retardation process (see Eq. (18)). The frequency-dependent phase shift between pressure and density leads to irreversible losses of wave energy. However, the properties of the medium are still reversible. It means that after a wave has passed through, the medium returns back to its equilibrium position. On the contrary, a passing wave in a *hysteretic* medium form residual stresses and strains, and the behavior of both wave and medium are irreversible. The loading and unloading follow different paths in the stress-strain diagram even at very low rates of deformation. In a usual medium without hysteresis, such slow processes are in thermodynamical equilibrium. But in hysteretic media, for example in metals, the nonlinear loading is associated with the accumulation of essentially irreversible plastic deformations and the unloading is close to linear. In materials characterized by destructive pseudo-elasticity (e.g., reinforced plastics with stress concentrated around fiber bends, cracks), unloading results in closure of some cracks and the unloading curve approaches the origin $\sigma = e = 0$,[19] where σ is the stress and e is the strain.

Crack "healing" occurring deformation processes was observed, for example, in concrete,[20,21] and creation and annihilation of a single defect was observed in metals.[21]

A Rayleigh hysteresis model of the stress-strain relationship is convenient, because of its simplicity, in describing quasi-static cyclic processes. Such a hysteretic loop, shown in curve 1 in Fig. 4, is described by the formulas

$$\begin{aligned}\sigma_- &= (E+\delta\, e_m)\, e + \frac{\delta}{2}\left(e^2 - e_m^2\right)\ ,\\ \sigma_+ &= (E+\delta\, e_m)\, e - \frac{\delta}{2}\left(e^2 - e_m^2\right).\end{aligned} \qquad (27)$$

The + sign in Eq. (27) corresponds to the upper branch of the loop in Fig. 4, and the – sign to the lower curve. The maximum and minimum values of strain are $\pm e_m$ and E is the Young modulus. The residual stress and hysteretic loss per cycle are given by the following expressions

$$\sigma_{RES} = \frac{\delta}{2}e_m^2\,, \quad U = \oint e\, d\sigma = \frac{4}{3}\delta e_m^3. \qquad (28)$$

However, model (27) is valid only for slow processes. The hysteretic loss determined by the loop area in Fig. 4 decreases with increase in frequency, because the internal processes (appearance of micro cracks, stress-induced dislocation birth, and motion) get frozen. The internal dynamics is similar to the one described by the Mandelstam-Leontovich relaxation theory (see

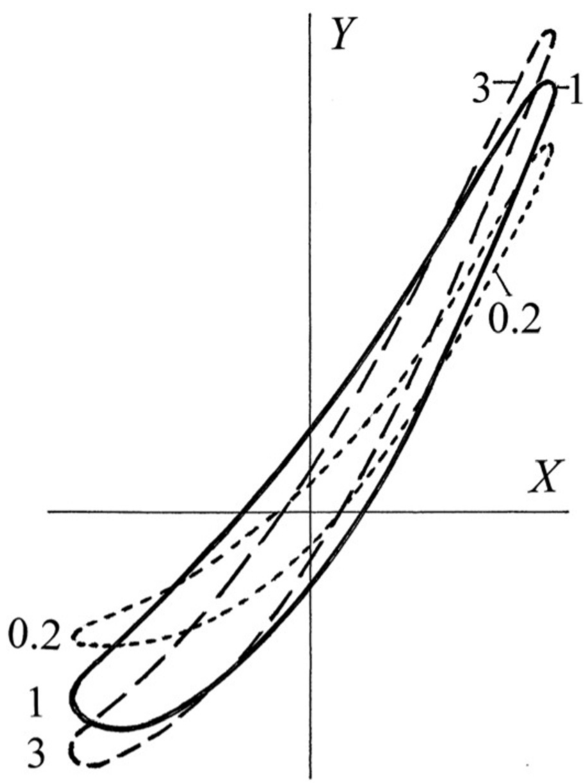

FIG. 3. The shape of cycles at $p' \Leftrightarrow \rho'$ diagram for a harmonic signal in a relaxing medium. The dotted, solid and dashed curves correspond to the following $\omega\tau$: 0.2, 1, and 3.

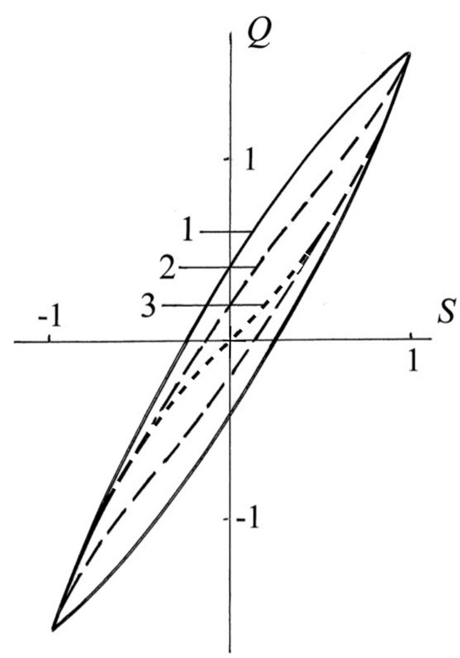

FIG. 4. The shape of cycles at $\sigma \Leftrightarrow e$ diagram for harmonic signal in hysteretic medium. Curves 1, 2, and 3 correspond to following magnitudes of frequency by nonlinear relaxation time $\omega\tau$: 0, 0.25, and infinity.

Ref. 2). In that theory, however, a *linear* internal parameter undergoes relaxation, approximating an equilibrium value in its own characteristic time τ. One could say, a relaxing medium has a *linear memory* with respect to acoustic disturbances (see Eq. (18)). In contrast, hysteretic media have *nonlinear memory*—keeping a memory of the acoustic wave through irreversible deformations and residual stresses proportional to e_m^2 (28), and this memory also has its own typical time scale τ.

The nonlinear hereditary model was developed in Ref. 22 to describe a soil-like medium compacted by a single wave. As distinct from the linear integral (18) with retarded kernel, the internal dynamics was described by the nonlinear integral term[14]

$$\frac{\rho'}{\rho_0}=\frac{p'}{c_0^2\rho_0}-\varepsilon\left(\frac{p'}{c_0^2\rho_0}\right)^2+\frac{\varepsilon}{c_0^4\rho_0^2\tau}\int_{t_m}^{t}K(t-t')[p'(x,t')-p_m(x)]^2dt'. \quad (29)$$

Here $p_m(x)$ is the maximum of acoustic pressure, reached at $t=t_m(x)$.

Similar generalization transforms the Rayleigh hysteresis (27) to the following pair of defining relationships

$$\sigma_{\pm}=eE\mp\delta e^2\pm\frac{\delta}{2\tau}\int_{t_m}^{t}K(t-t')[e(t')\pm e_m]^2dt'. \quad (30)$$

The upper signs in Eq. (30) corresponds to the upper branch of the loop in Fig. 4 and the lower signs to the lower branch.

The curves in Fig. 4 are constructed with the exponential kernel (19) and for a harmonic strain vibration (9). At small frequencies $\omega\tau<1$, the following approximate formula is derived

$$Q_{\pm}=\left(\frac{E}{e_m}+\delta\right)S\pm\frac{\delta}{2}\left(1-S^2\right)\mp\delta\omega\tau(1\pm S)\sqrt{1-S^2}, \quad (31)$$

where $Q=\sigma/e_m^2$ and $S=e/e_m$, because at arbitrary ωt, a parametric representation is more convenient.

The curves 1, 2, and 3 in Fig. 4 correspond to three different frequencies of the acoustic wave: $\omega\tau=0$, $\omega\tau=0.25$, and $\omega\tau\to\infty$. Curve 1 represents the equilibrium Rayleigh hysteresis (27). With increase in frequency, the hysteretic loop shrinks and its area tends to zero at very high frequencies (see curve 3).

It is possible to derive a differential equation from the integro-differential one for an exponential kernel (19). To do this, the integral relation (30) is rewritten in a differential form

$$\left(\frac{d}{dt}+\frac{1}{\tau}\right)\sigma=\frac{df(e)}{dt}+\frac{g(e)}{\tau}. \quad (32)$$

Formula (32) is more general than (30). As follows from (32), at high frequencies $\omega\tau\to\infty$, the stress σ tends to the arbitrary function $f(e)$ — for example, to the solid central curve 3 in Fig. 4. It also follows from (32), that at low frequencies $\omega\tau\to 0$, the stress σ tends to the second arbitrary function $g(e)$. It must have two branches $g_{\pm}(e)$ (like Eq. (27)) in order to describe the hysteresis loop. And all three functions, $f(e)$ and $g_{\pm}(e)$ must be coincident at both ends (at $e=\pm e_m$).

By using the wave equation connecting σ and e

$$\rho_0\frac{\partial^2 e}{\partial t^2}=\frac{\partial^2\sigma}{\partial x^2}, \quad (33)$$

and by defining Eq. (32), a single nonlinear wave equation can be derived for the strain e

$$\left(\frac{\partial}{\partial t}+\frac{1}{\tau}\right)\left(\frac{\partial^2 e}{\partial t^2}-c^2\frac{\partial^2 e}{\partial x^2}\right)=\frac{\partial^2}{\partial x^2}\left(\frac{\partial F(e)}{\partial t}+\frac{G_{\pm}(e)}{\tau}\right). \quad (34)$$

The functions F,G are connected to f,g through

$$\rho_0F(e)=f-Ee,\qquad \rho_0G_{\pm}=g_{\pm}-Ee. \quad (35)$$

Consequently, the left-hand-side of Eq. (34) consists of linear terms, and the nonlinear ones are collected in the right-hand side.

For acoustic waves, the nonlinearity is usually weak. Then a simplified evolution equation can be derived from Eq. (34) by means of the asymptotic method of slowly varying wave profile.[11] Transforming it to new coordinates $x,\xi=t-x/c$, where $c=\sqrt{E/\rho_0}$ is the rod sound velocity, we derive

$$\left(\frac{\partial}{\partial\xi}+\frac{1}{\tau}\right)\frac{\partial e}{\partial x}=-\frac{1}{2c}\frac{\partial}{\partial\xi}\left(\frac{\partial F(e)}{\partial\xi}+\frac{G_{\pm}(e)}{\tau}\right). \quad (36)$$

The solutions to the pair of nonlinear equations (36) must be sewn together in the points $\tau_{m\pm}(x)$ where the strain reaches the extreme values $\pm e_m(x)$ of the cycle, by analogy with the approach used in Ref. 22.

These Eqs. (34) and (36), explain the slow dynamic phenomena[23] observed in resonator experiments.[24] Their solution describing nonlinear standing waves can be derived by the asymptotic methodology developed before for high-power resonant vibrations.[25,26]

V. DISCUSSION

For clarification of the results above, a discussion is desirable. In accordance with a classification given in Ref. 20, the known types of acoustic nonlinearity are divided into 2 classes: volume (V) and boundary (B) nonlinearity. In turn, each of these classes is subdivided in 3 groups: physical (P), geometrical (G), and structural (S) nonlinearity. For example, BP means "boundary physical" nonlinearity, and VS means "volume structural" one. Examples of these are given in Ref. 20.

It is also necessary to distinguish between the terms "strong nonlinearity" and "strongly expressed nonlinearity" which are often used interchangeably. As a rule, most acoustic problems are weakly nonlinear, because the acoustic Mach number is small ($M\ll 1$). The Mach number M is the ratio of the particle velocity u and the speed of sound c_0, or the ratio of the acoustic pressure and the characteristic internal pressure of a medium $c_0^2\rho_0$. However, these weak volume nonlinear effects can accumulate during long-distance propagation and lead to strongly expressed phenomena like shock front formation or significant energy flow to new spectral regions.

Strong nonlinearity appears commonly at Mach numbers exceeding unity. Some well known phenomena are explosive waves, high-speed impacts, and cavitation, which are often accompanied by destruction of the medium. Sometimes strongly nonlinear unusual phenomena appear. One example is structures with bonds limiting the mobility of particles so that they have no transition to the infinitesimally weak linear limit.[27] Another example is the "clapping" nonlinearity of non-pre-pressured Hertz contacts typical for grainy media.[28] Such types as boundary structural (BS) and VS display strongly nonlinear properties even at small deformations.[20]

It is appropriate to cite a few selected papers on hereditary and hysteretic materials.[29–33] The great number of existing papers is caused by the wide variety of real materials used in geophysics and industry. Even for each individual material subjected to quasi-static loading, the kernels of the Volterra-Frechet series describing the hereditary properties can rarely be reconstructed because of deficiency of data.[19] In addition to variations in the low-frequency behavior, these kernels display diversified dispersion or dependence on high acoustic frequencies. The analogous problems in optics[14] are solved by linear and nonlinear laser spectroscopy which provides data for reconstruction of kernels of susceptibility. Similar approaches can be used in acoustics and mechanics.

VI. CONCLUSIONS

Pressure-density loops have been presented as images of dissipative and hysteretic irreversible processes in linear and nonlinear acoustic fields. New equations were presented describing the slow dynamic processes, and types of relevant nonlinearities were defined.

The theory developed here is important for several problems in applied physics. For example, it can be used to evaluate and compare different mechanisms of losses of high-intensity vibrations and waves. It can support also one of the frontiers of applied studies, namely, the nonlinear nondestructive testing of materials displaying unusual behavior like slow dynamics,[23,24] by measuring typical times of linear and nonlinear relaxation and dynamic strength. Detailed comparisons between this theory and experimental data will be performed and published later.

ACKNOWLEDGEMENTS

This work is supported by the Knowledge Foundation (KKS, Sweden), BTH, the RFBR, and the Presidential Program for Leading Scientific Schools.

[1] L. Bergmann, *Der Ultraschall und Seine Anwendung in Wissenschaft und Technik* (S. Hirzel Verlag, Zürich, 1954).
[2] L. D. Landau and E. M. Lifshitz, *Fluid Mechanics* (Pergamon, Oxford, 1986).
[3] O.V. Rudenko and S. I. Soluyan *Theoretical Foundations of Nonlinear Acoustics* (Consultants Bureau, New York, Plenum, 1977).
[4] R. T. Beyer, *Nonlinear Acoustics* (AIP, New York, 1997).
[5] *Nonlinear Acoustics*, edited by M. F. Hamilton and D. T. Blackstock (Academic, San Diego, 1997).
[6] K. A. Naugolnykh and L. A. Ostrovsky, *Nonlinear Wave Processes in Acoustics* (Cambridge University Press, New York, 1998).
[7] B. O. Enflo and C. M. Hedberg, *Theory of Nonlinear Acoustics in Fluids* (Kluwer, Dordrecht, 2002).
[8] S. I. Soluyan and R. V. Khokhlov, Vestn. Mosk. Univ., Fiz., Astron. (Moscow Univ. Phys. Bull.) **52**, 31 (1961).
[9] R. V. Khokhlov and S. I. Soluyan, Acustica **14**, 242 (1964).
[10] R. V. Khokhlov, To the theory of shock radiowaves in nonlinear lines. Sov. Phys.- Radiotech. Electron. **6**(6), 917 (1961).
[11] O. V. Rudenko, S. N. Gurbatov, and C. M. Hedberg, *Nonlinear Acoustics through Problems and Examples* (Trafford, Victoria, 2010).
[12] O. V. Rudenko, Physics-Uspekhi (Adv. Phys. Sci.) **38**(9), 965 (1995).
[13] O. V. Rudenko, S. I. Soluyan, and R. V. Khokhlov, "Problems of the theory of nonlinear acoustics," in *Finite-Amplitude Wave Effects in Fluids* (IPC Science and Technology Press, London, 1974). See also Sov. Phys. Acoust. **20**(3), 356 (1974).
[14] M. B. Vinogradova, O. V. Rudenko, and A. P. Sukhorukov, *Theory of Waves*, 2nd ed. (Nauka Publishers, Moscow, 1990).
[15] A. P. Sarvazyan, O.V. Rudenko, S. D. Swanson, J. B. Folwkes, and S. Y. Emelianov, Ultrasound Med. Biol. **24**(9), 1419 (1998).
[16] O. V. Rudenko and K. L. Khirnykh, Sov. Phys. Acoust. **36**(3), 293 (1990).
[17] O. V. Rudenko and A. P. Sarvazyan, Acoust. Phys. **52**(6), 833 (2006).
[18] P. V. Lebedev-Stepanov and O. V. Rudenko, Acoust. Phys. **55**(6), 729 (2009).
[19] Yu. N. Rabotnov, *Elements of Hereditary Solid Mechanics* (Mir Publishers, Moscow, 1980).
[20] O. V. Rudenko, Phys. Usp. (Adv. Phys. Sci.) **49**(1), 69 (2006).
[21] M. Yu. Izosimova, A. I. Korobov, and O. V. Rudenko, Acoust. Phys. **55**(2), 153 (2009).
[22] O. V. Rudenko and V. A. Robsman, Acoust. Phys. **50**(6), 725 (2004).
[23] R. A. Guyer and P. A Johnson, Phys. Today **52**, 30 (1999).
[24] K. C. E. Haller and C. M. Hedberg, Phys. Rev. Lett. **100**, 068501 (2008).
[25] B. O. Enflo, C. M. Hedberg, and O. V. Rudenko, J. Acoust. Soc. Am. **117**(2), 601 (2005).
[26] O. V. Rudenko, Acoust. Phys. **55**(1), 27 (2009).
[27] O. V. Rudenko and E. V. Solodov, Acoust. Phys. **57**(1), 51 (2011).
[28] O. V. Rudenko and C. M. Hedberg, Nonlinear Dyn. **35**, 187 (2004).
[29] K. R. McCall and R. A. Guyer, J. Geophys. Res. **99**(B12), 23887 (1994).
[30] H. Xu, S. M. Day, and J.-B. H. Minster, J. Geophys. Res. **103**(B12), 29915 (1998).
[31] O. O. Vakhnenko, V. O. Vakhnenko, and T. J. Shankland, Phys. Rev. B **71**, 174103 (2005).
[32] V. O. Vakhnenko, O. O. Vakhnenko, J. A. TenCate, and T. J. Shankland, Phys. Rev. B **76**, 184108 (2007).
[33] H. Xu, S. M. Day, and J.-B. H. Minster, Bull. Seismol. Soc. Am. **89**(4), 903 (1999).